UC Riverside

UC Riverside Previously Published Works

Title

Machine learning model to predict evolution of pulseless electrical activity during in-hospital cardiac arrest.

Permalink

https://escholarship.org/uc/item/0mt924m9

Authors

Urteaga, Jon

Elola, Andoni

Norvik, Anders

et al.

Publication Date

2024-03-01

DOI

10.1016/j.resplu.2024.100598

Peer reviewed

Clinical paper

Machine learning model to predict evolution of pulseless electrical activity during in-hospital cardiac arrest

Jon Urteaga [a], Andoni Elola [b], Anders Norvik [c], Eirik Unneland [c], Trygve C. Eftestøl [d], Abhishek Bhardwaj [e], David Buckler [f], Benjamin S. Abella [g], Eirik Skogvoll [c], Elisabete Aramendi [a,h,*]

Abstract

Background: During pulseless electrical activity (PEA) the cardiac mechanical and electrical functions are dissociated, a phenomenon occurring in 25–42% of in-hospital cardiac arrest (IHCA) cases. Accurate evaluation of the likelihood of a PEA patient transitioning to return of spontaneous circulation (ROSC) may be vital for the successful resuscitation.

The aim: We sought to develop a model to automatically discriminate between PEA rhythms with favorable and unfavorable evolution to ROSC.

Methods: A dataset of 190 patients, 120 with ROSC, were acquired with defibrillators from different vendors in three hospitals. The ECG and the transthoracic impedance (TTI) signal were processed to compute 16 waveform features. Logistic regression models where designed integrating both automated features and characteristics annotated in the QRS to identify PEAs with better prognosis leading to ROSC. Cross validation techniques were applied, both patient-specific and stratified, to evaluate the performance of the algorithm.

Results: The best model consisted in a three feature algorithm that exhibited median (interquartile range) Area Under the Curve/Balanced accuracy/Sensitivity/Specificity of 80.3(9.9)/75.6(8.0)/ 77.4(15.2)/72.3(16.4) %, respectively.

Conclusions: Information hidden in the waveforms of the ECG and TTI signals, along with QRS complex features, can predict the progression of PEA. Automated methods as the one proposed in this study, could contribute to assist in the targeted treatment of PEA in IHCA.

Keywords: Pulseless electrical activity (PEA), Machine Learning models, Cardiopulmonary resuscitation (CPR), Evolution prediction

Introduction

The cardiac electrical activity with no effective mechanical contractions (PEA) is a rhythm frequently present in cardiac arrest, with recorded prevalence of 20–30% in out-of-hospital (OHCA) and up to 40–60% in in-hospital cardiac arrest (IHCA).[1–3] In recent decades, PEA prevalence in IHCA increased from 36% in 2000 to 46% in 2009,[4] and similar increasing trends were observed in out-of-hospital studies.[5–7]

In the context of cardiopulmonary resuscitation (CPR), biosignals as electrocardiogram (ECG) and thoracic impedance (TTI) provide valuable information that can assist identifying the prognosis of PEA and guide the appropriate treatment towards the return of spontaneous circulation (ROSC).[8,9] Knowledge of the prognosis of PEA can help clinicians make informed decisions about the appropriate treatment and management of patients,[10,11] discriminating favorable from unfavorable PEA. Pseudo-PEA rhythms show small mechanical activity, albeit insufficient for a palpable pulse, in contrast to

true-PEA with no mechanical cardiac activity.[8,12,13] The two types of PEA have different prognosis and treatment,[13–16] and their distinction is of great clinical interest to predict the hemodynamical evolution of PEA and their outcome.

Both heart rate (HR) and QRS complex duration are biomarkers that are readily accessible during both the initial and subsequent rhythm assessments. Recent studies have indicated their relation with the outcome and suggest that HR increase and QRS duration decrease indicate a higher probability of ROSC.[10,17–19] More sophisticated features of the ECG and the TTI computed in the frequency domain, as AMSA and the cross-power between ECG and TTI signals, have also shown the potential to predict ROSC.[9] Their combinations in machine learning (ML) models have been proposed to predict the immediate rhythm transition during cardiac arrest,[20] to classify different types of rhythm,[21] and to distinguish between favorable (faPEA) and unfavorable (unPEA) PEA, the former denoting instances of PEA evolving into sustained ROSC (minimum 20 min), while the latter pertaining to PEA cases wherein pulse is not regained.[9,22]

In this study multivariable machine learning models have been proposed to discriminate PEAs with favorable prognosis in IHCA. Features based on different signals and QRS complexes have been included in an automated model, in addition to a new version of the Amplitude Spectrum Area. The potential of the ECG and TTI features, hidden in the biosignal waveforms, were analyzed and combined in a sophisticated regression based classifier. Retrospective analysis of IHCA episodes permitted the evaluation of the accuracy of the models.

Materials and methods

Data materials

The data used in this study was a subset of a larger database containing IHCA episodes from different hospitals. The subset comprised of 197 episodes recorded by emergency services: 83 episodes from St. Olav University Hospital (Trondheim,Norway), 90 episodes from the Hospital of the University of Pennsylvania (USA) and 24 episodes from Penn Presbyterian Medical Center (USA). The episodes from Norway, captured between 2018 and 2021, were recorded using Lifepak- 20 defibrillators (Stryker, Redmond, USA), whereas the episodes from Pennsylvania, captured between 2008 and 2010, were recorded using HeartStart MRx-defibrillators (Philips Medical Systems, Andover, Massachusetts, USA). Out of 197 episodes, 190 came from different patients, and a summary of the patient cohort's characteristics is presented in Table 1.

The median (Interquartile range, IQR) duration of the episodes was 17.1 (9.1–32.2) min from the start of the episode to the ROSC/end-of-CPR, and in 120 episodes sustained ROSC was achieved, 8.2(5.3–19.9) min after switching on the defibrillator. Sustained ROSC was defined as a pulsed rhythm with no chest compressions at least during 20 min.[7]

Expert clinicians reviewed and manually annotated all episodes. They annotated rhythm type and QRS complexes in the ECG signal, and identified chest compression series in the TTI. For the analysis, PEA segments of 5 s duration, separated by at least 1 s, were extracted during chest compression pauses. As rates below 12 bpm during longer than 5 s are considered asystole, a minimum duration of 5 s and 12 bpm were demanded to guarantee that all segments were PEA rhythms.[23–25] Fig. 1 shows two examples of the

Table 1 – Summary of patient and episode statistics. Data are presented as percentage or median (Interquartile range, IQR).	
Patient Summary (*n* = 190)	
Metric	Value
Age (years)	69.5 (57.8–77.3)
Male gender	54.2%
Survived to discharge	17%
Episode Summary (*n* = 197)	
Metric	Value
Monitored CA	78%
Assumed cardiac cause	55%
Received adrenaline	84%

dataset, where both the ECG and the TTI signals are represented with some meaningful features.

Methods

This section described the procedure to define the PEA analysis based on ML models. The method is divided in three stages consisting of: 1) Preprocessing of ECG and TTI signals, 2) Feature characterization of the signals, and 3) Design of feature-based ML models for binary classification. This last stage includes the training/validation of the models as well as their statistical characterization.

ECG and TTI preprocessing

ECG and TTI signals were preprocessed following the scheme proposed in a previous study.[9,22] The ECG signal was denoised using a stationary wavelet transform (SWT) technique. This involved applying a band-pass filter in the band of 0.5–31.25, Hz to remove baseline noise, high-frequency noise, motion artifacts, and ventilation artifacts. The impedance circulation component (ICC), which reflects the ventricular contractions in the TTI signal correlated with ECG heartbeats,[22,26] was extracted from the TTI signal and filtered 1–8 Hz.[9,22] In Fig. 1, it can be observed how the ICC component of TTI signal correlated with the QRS complexes in the ECG.

Feature extraction

The sets of features considered in this study were gathered in three groups: The ECG and ICC waveform features, previously proposed in cardiac arrest studies, and new additional QRS related features.

ECG waveform features

The main ECG waveform computed, non QRS specific features, were the following:

- The Amplitude Spectrum Area (AMSA) was calculated by summing the product of the spectral amplitudes and corresponding frequencies in the band of 2–48 Hz of the ECG signal as proposed in.[27] It has been widely reported as a reliable predictor for successful defibrillation, and it is indicative of both coronary perfusion pressure and myocardial energy state.[9,28,29]
- ModAMSA is a modified version of AMSA that calculates the spectral content in the frequency range of 20–30 Hz. The Mod-AMSA associated to faPEA rhythms was observed to be higher than the value for unPEA. The Figure in Appendix A shows
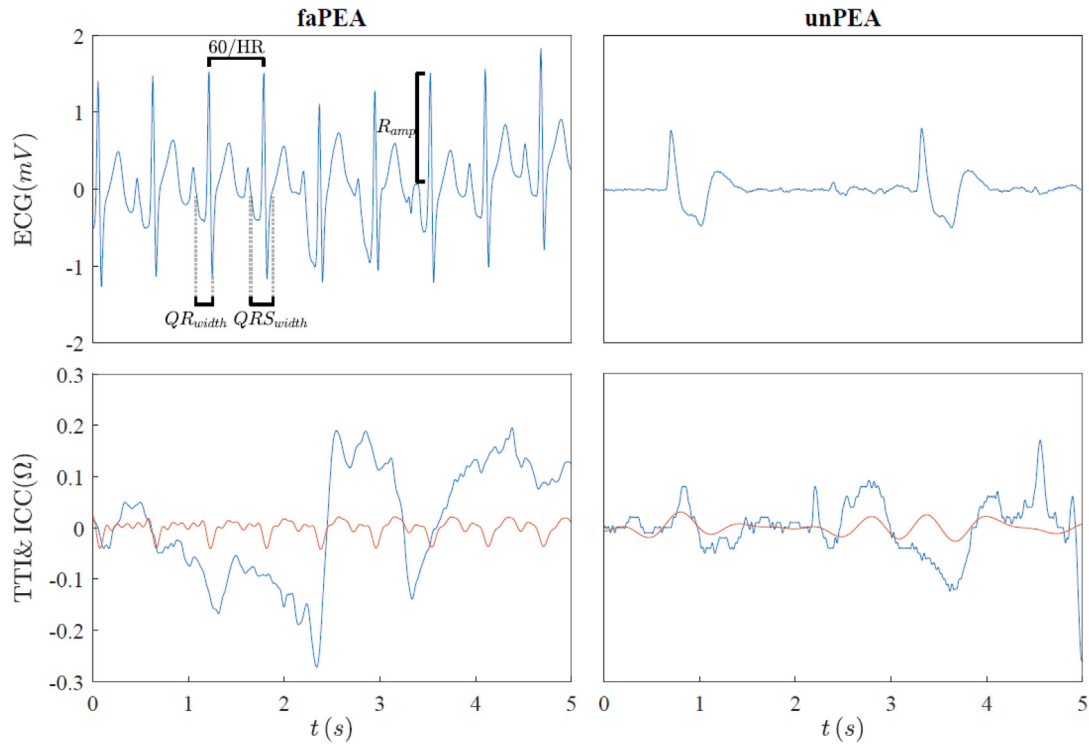
Fig. 1 – Two PEA cases corresponding to faPEA (left) and unPEA (right) are shown. On the top the ECG signals, with HR$_{mean}$, QR$_{width}$, QRS$_{width}$, and R_{amp} represented. On the bottom the TTI and the computed impedance circulation component, ICC, in red.

how the spectral content of both types of rhythms overlaps considerably between 0 and 15 Hz but becomes more distinct between 20 and 30 Hz.

- The Smoothed Nonlinear Energy Operator(SNEO) computed in the ECG, SNEO$_{ECG}$, measures the local energy content of the ECG signal as described in.[30] It has been classically applied for QRS complex detection, [31] shock outcome prediction[30] and identification of circulatory status.[22]
- The Autoregressive Burg's value (ARB) computed in the ECG signal, ARB$_{ECG}$, evaluates the similarity between the power spectral density of the signal with an autoregressive model of the spectrum.[32] It has been used for identification of circulatory status[22], cardiac rhythm classification[33] and prediction of prognosis of PEA during OHCA.[9]
- Entropy is a complexity measure that quantifies the regularity of the ECG.[34]

ICC waveform features

The ICC of the TTI was computed as described in[9,22] and features computed as follows:

- Cross$_{Power}$ is the cross power between the ECG and ICC signals. High Cross$_{Power}$ indicates pulsatile rhythms, and it has been proposed for automatic circulation detection in OHCA. [35]
- LogPower$_{ICC}$ is the logarithmic energy of the ICC signal, which is related to the ventricular wall movement.[36]
- SNEO$_{ICC}$ is the SNEO value of the ICC signal, computed as described in section 3.2.1.

- ARB$_{ICC}$ is the ARB of the ICC signal, computed as described in section 3.2.1.

QRS waveform features

Additionally to ECG waveform features, several metrics related to the QRS waveform were computed using the manual annotations of the Q, R, and S waves made by clinicians.

- HR$_{mean}$ and HR$_{var}$ are the mean and variance values of HR, respectively, computed as the inverse of consecutive R-R intervals.
- QRS$_{width}$ and QR$_{width}$ correspond to the durations of Q-S and Q-R complex, respectively.
- QRS$_{slope}$ and QR$_{slope}$ are computed as the sum of the amplitude values of QRS and QR complexes in the first difference signal divided by QRS$_{width}$ and QR$_{width}$, respectively.
- R$_{amp}$ is the mean value of the amplitude of the R wave peaks in the segment.

A detailed description of the algorithms applied to compute the features can be found in Appendix B.

LR classifier

A logistic regression model (LR) was used to classify PEA segments into faPEA or unPEA. The models were trained and tested combining multiple variables. LR was the best option to make understandable binary classifications. The probability of a segment to be a faPEA was computed following the next equation[36]:

$$p = \frac{1}{1 + e^{-z}}$$

where z is the linear combination of the independent features weighted by their coefficients:

$$z = \beta_0 + \beta_1 x_1 + \beta_2 x_2 + \dots + \beta_n x_n$$

In this equation, β_0, β_1, β_2, ..., β_n are the regression coefficients estimated during the model fitting process, and x_1, x_2, ..., x_n are the features of the PEA segment.

The maximum Area Under the ROC Curve (AUC) was applied as the optimization criteria in the design process.

Feature selection has been performed using forward feature selection. This means that we started with the feature with the highest AUC, and at each step, we added the feature that, when combined, provided the best AUC.

Validation

A 10-fold cross-validation (CV) technique was used for model validation, using different sets of patients for training and testing. This implies that all segments extracted from a patient were used either for training or for testing within each fold; segments from the same patient were never split for training and testing the model. To improve reliability, the partition was done assigning the same weight to all patients, which avoided data leakage between folds.

The performance of the classifiers was evaluated using standard performance metrics for binary classifiers, with faPEA as the positive class. The AUC, Sensitivity (Se), Specificity (Sp) and Balanced Accuracy (BAC, the average of Se and Sp) were considered as the performance metrics.

The performance metric that was primarily focused on optimizing in this study was the AUC.

Time analysis

In previous studies on rhythm evolution or pulse detection in cardiac arrest, predictability was shown to vary over time.[7,9,37,38] In this second analysis segments were separated in four groups (quartiles) depending on their time distance to the ROSC/end-of-CPR, and models analyzed in terms of proximity to the end. While maintaining the 10-fold CV architecture, the models were trained using segments from all quartiles and performance was evaluated in each specific quartile.

Additionally, the evolution of the top three features was analyzed over the last 15 minutes of the episode, and an exponential function adjusted to characterize their evolution.

Results

A total of 1468 PEA segments of 5 s duration were extracted from 197 episodes, with a median (IQR) of 4(1–8) segments per episode. The segments observed during episodes with ROSC were categorized as faPEA, while those without ROSC were categorized as unPEA. There was a total of 767 faPEA segments, median (IQR) 2 (1–9) per episode, and 701 unPEA segments, 5 (3–9) per episode. The 25th, 50th, and 75th percentiles of their time to ROSC/end-of-CPR were 180, 383, and 772 seconds, respectively.

In Table 2, the independent analysis of each feature can be observed for faPEA/unPEA groups. The median (IQR) value of each

Table 2 – Median (IQR) values of each feature for faPEA and unPEA segments are shown, the AUC of the LR classifier. Mann-Whitney U-test was performed considering one value (median among segments) per feature and per patient.

Feature	faPEA	unPEA	AUC(%)	p-value
ECG Features				
AMSA	24.50 (16.56–39.32)	14.00 (9.47–20.50)	75.23 (69.42–81.82)	$3.5 \cdot 10^{-4}$
ModAMSA	4.14 (2.15–6.93)	1.52 (0.94–2.51)	79.13 (74.59–85.72)	$8.3 \cdot 10^{-6}$
$SNEO_{ECG}$	0.16 (0.04–0.65)	0.07 (0.01–0.23)	63.78 (55.81–71.68)	$6.8 \cdot 10^{-5}$
ARB_{ECG}	$2.18 \cdot 10^{-6}$ ($0.71 \cdot 10^{-6}$ $-4.57 \cdot 10^{-6}$)	$0.48 \cdot 10^{-6}$ ($0.26 \cdot 10^{-6}$ $-1.15 \cdot 10^{-6}$)	77.89 (73.47–84.47)	$1.4 \cdot 10^{-9}$
Entropy	0.29 (0.21–0.35)	0.22 (0.16–0.31)	63.06 (57.69–70.45)	$9.6 \cdot 10^{-3}$
TTI Features				
$Cross_{Power}$	0.51 (0.14–1.24)	0.30 (0.07–0.80)	58.93 (54.31–64.19)	$4.8 \cdot 10^{-3}$
$LogPower_{ICC}$	4083 (2518–5412)	3308 (1673–4412)	59.54 (55.37–64.83)	$2.1 \cdot 10^{-3}$
$SNEO_{ICC}$	$1.1 \cdot 10^{-3}$ ($0.17 \cdot 10^{-3}$ $-4.65 \cdot 10^{-3}$)	$0.48 \cdot 10^{-3}$ ($0.11 \cdot 10^{-3}$ $-1.80 \cdot 10^{-3}$)	59.99 (55.56–64.34)	$4.3 \cdot 10^{-2}$
ARB_{ICC}	$43.36 \cdot 10^{-9}$ ($4.81 \cdot 10^{-9}$ $-340.91 \cdot 10^{-9}$)	$27.51 \cdot 10^{-9}$ ($5.76 \cdot 10^{-9}$ $-113.21 \cdot 10^{-9}$)	57.53 (54.16–64.93)	$2.4 \cdot 10^{-2}$
QRS Features				
HRmean	74.26 (46.57–113.40)	70.83 (38.11–90.40)	56.48 (52.51–62.31)	$2.2 \cdot 10^{-2}$
HR_{var}	5.14 (0.41–157.79)	6.77 (0.06–101.21)	57.75 (55.42–62.98)	$1.2 \cdot 10^{-2}$
QRSwidth	155 (113–195)	205 (160–262)	68.74 (60.92–77.76)	$6.6 \cdot 10^{-5}$
QRwidth	52 (40–77)	67 (50–97)	65.31 (56.35–73.33)	$2.3 \cdot 10^{-3}$
Ramp	0.36 (0.04–0.70)	0.19 (0.23–0.40)	63.29 (57.29–68.74)	$1.0 \cdot 10^{-2}$
QRS_{slope}	0.013 (0.009–0.019)	0.007 (0.005–0.011)	77.63 (68.41–82.08)	$4.3 \cdot 10^{-7}$
QRslope	0.011 (0.008–0.017)	0.007 (0.005–0.096)	72.43 (65.91–78.91)	$2.0 \cdot 10^{-6}$

type of segments was computed using the whole dataset, while AUC was computed following the 10-fold CV model explained in methods section. The results in terms of discrimination power are quite aligned with previous OHCA analysis for ECG and TTI signals,[9] showing AUC values above 75% in several single features.

All the features showed different medians for unPEA and faPEA groups according to Mann-Whitney U-test ($p < 0.05$). However, the features that showed lowest p values, with $p < 0.005$, were Mod-AMSA, AMSA, $SNEO_{ECG}$, ARB_{ECG}, $LogPower_{ICC}$, $Cross_{Power}$, QRS_{width}, QR_{width}, QRS_{slope} and QR_{slope}.

The performance of the LR classifiers in terms of the number of features, following the criteria of forward feature selection explained in the methods section, is shown in Table 3. The analysis revealed that the best performance was achieved with a three-feature model based on: ModAMSA, $LogPower_{ICC}$, QRS_{width}, with AUC/BAC values of 80.3% and 75.6%, respectively. No improvement was observed increasing the number of features.

In the time analysis, the performance of the three-feature LR model was analyzed in terms of the distance to the ROSC/end-of-CPR and results are shown in Fig. 2. It can be observed that the classifier performs better for segments closer to the end (Q4 compared to Q1). Specifically, the Q4 group with a time-distance of 0–180 s from the end showed an AUC/BAC of 87.3%/BAC of 79.1%, while the Q1 at > 772 s from the end presented AUC/BAC of 69.6%/59.9%.

To better understand the results, we analyzed the evolution of the top three features in the last 15 minutes before ROSC. Fig. 3 shows that the values of ModAMSA, QRS_{width} and ICC log Power separate for faPEA(blue) compared to unPEA(red) further as ROSC approaches. These results confirm the potential of these features to evaluate the proximity to ROSC and discriminate between PEA with favorable and unfavorable prognosis.

The study also confirms previous findings[9,10,17–19] that as PEA episodes progress, the predictability of PEA prognosis increases. This is supported by the results in Fig. 2, as well as the observation that features of each type become increasingly distinct over time, as seen in Fig. 3.

Discussion

This work presents a novel predictive model that integrates ECG and TTI features to discriminate PEAs with positive prognosis. This is the first time such a model is designed for IHCA patients and integrates QRS specific features.

The application of ML models to design predictive models for IHCA reinforce previous conclusions of Urteaga et al. with OHCA.[9] Both studies highlight the importance of feature selection and integration of different sources of information to develop accurate tools for PEA state evolution prediction in cardiac arrest patients.

In contrast to previous automated methods, this study integrates QRS complex features that have demonstrated great potential to predict the outcome of PEA.[10,17–19,39,40] The AUC obtained for the QRS complex duration is aligned with previous results, and combining QRS complex features with other ECG/ICC features has improved the overall performance of the model 0.6 points of AUC and 4.1 points of BAC. Fig. 3 showed that QRS complexes are narrower in faPEA segments compared to unPEA, and that they evolve to narrower values as episode progresses towards ROSC. However, the discriminative power of HR does not support its use in this application (see Table 2).

Table 3 – The LR model's performance in terms of median (IQR) AUC, BAC, Se, and Sp. All possible combinations using one to six features have been tested, only the best for each number of features is shown.

	No. Features	AUC (%)	BAC (%)	Se (%)	Sp (%)
ModAMSA	1	79.1 (74.6–85.7)	71.4 (63.9–75.7)	62.9 (56.1–71.9)	79.2 (70.2–89.9)
ModAMSA + $LogPower_{ICC}$	2	79.7 (73.7–85.3)	71.5 (65.2–79.0)	64.2 (57.7–73.9)	78.5 (71.1–88.0)
ModAMSA + $LogPower_{ICC}$ + QRS_{width}	3	80.3 (73.3–85.7)	75.6 (69.6–80.1)	77.4 (70.3–84.2)	72.3 (61.9–79.6)
ModAMSA + $LogPower_{ICC}$ + QRS_{width} + ARB_{ECG}	4	80.2 (73.4–85.7)	75.5 (69.9–80.3)	77.5 (69.9–83.5)	69.5 (60.2–80.0)
ModAMSA + $LogPower_{ICC}$ + QRS_{width} + ARB_{ECG} + QR_{width}	5	79.8 (73.4–85.8)	73.1 (69.0–79.2)	77.8 (69.8–83.8)	66.4 (59.1–78.9)
ModAMSA + $LogPower_{ICC}$ + QRS_{width} + ARB_{ECG} + QR_{width} + $Cross_{Power}$	6	79.6 (73.3–85.7)	72.6 (68.9–72.3)	76.4 (68.7–82.9)	64.4 (58.6–77.7)
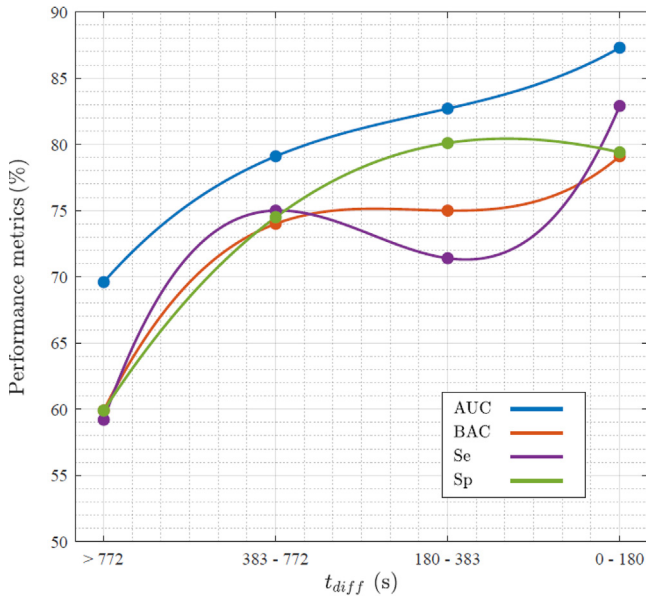
Fig. 2 – Performance of the LR model with three features for segments according to their distance from the ROSC/end-of-episode. The figure shows the median (IQR) values for AUC, BAC, Se and Sp.

The QRS_{width} and the HR are the characteristics that have been studied as indicators of PEA prognosis. Norvik et al. and Aufderheide et al. have found a correlation between QRS_{width} and HR with survival.[17,19,41] Both studies demonstrated that smaller QRS_{width} and higher HR are associated with more favorable outcomes in PEA.

On the other hand, Weisser et al. only found a correlation between HR and prognosis, not with QRS_{width}.[42] This is in contrast to Kim et al., who found a correlation with the duration of the QRS complex but not with HR.[40] In this study, the correlation of QRS_{width} with the prognosis of pulseless electrical activity (PEA) has been demonstrated. In Fig. 2, it can be observed how the mean value of QRS_{width} differs more as it approaches the ROSC/end-of-CPR. This is consistent with the results of Norvik et al.[19]

It is worth highlighting that ModAMSA, which is the independent feature that shows the best performance in Table 2, also exhibits the most significant difference over time in Fig. 2. High values of Mod-AMSA are associated with more content in the high-frequency spectrum, which is caused by high HR and narrow QRS complexes with high amplitude.

The results also demonstrate that ModAMSA, a modified version of the AMSA, has better predictive capabilities than the original feature to differentiate an unPEA from a faPEA. This finding highlights the potential of the frequency range of 20–30 Hz to classify PEA segments according to their prognosis. This frequency band has already shown potential for the detection and classification of cardiac rhythms in previous studies.[9,34,43] Other applications of AMSA[44–47] might benefit from this new definition and provide more accurate predictive models.

Regarding the number of features included in the predictive models, it can be concluded that more features do not necessarily improve the accuracy of the algorithm (see Table 3) because their contribution may result redundant or irrelevant to the model. In our case the best model was reached with three features, one from each group: ECG signal waveform, ICC signal waveform, and QRS complex shape. Each of these features also happens to have the highest AUC value among all the features that showed $p < 0.005$ within their
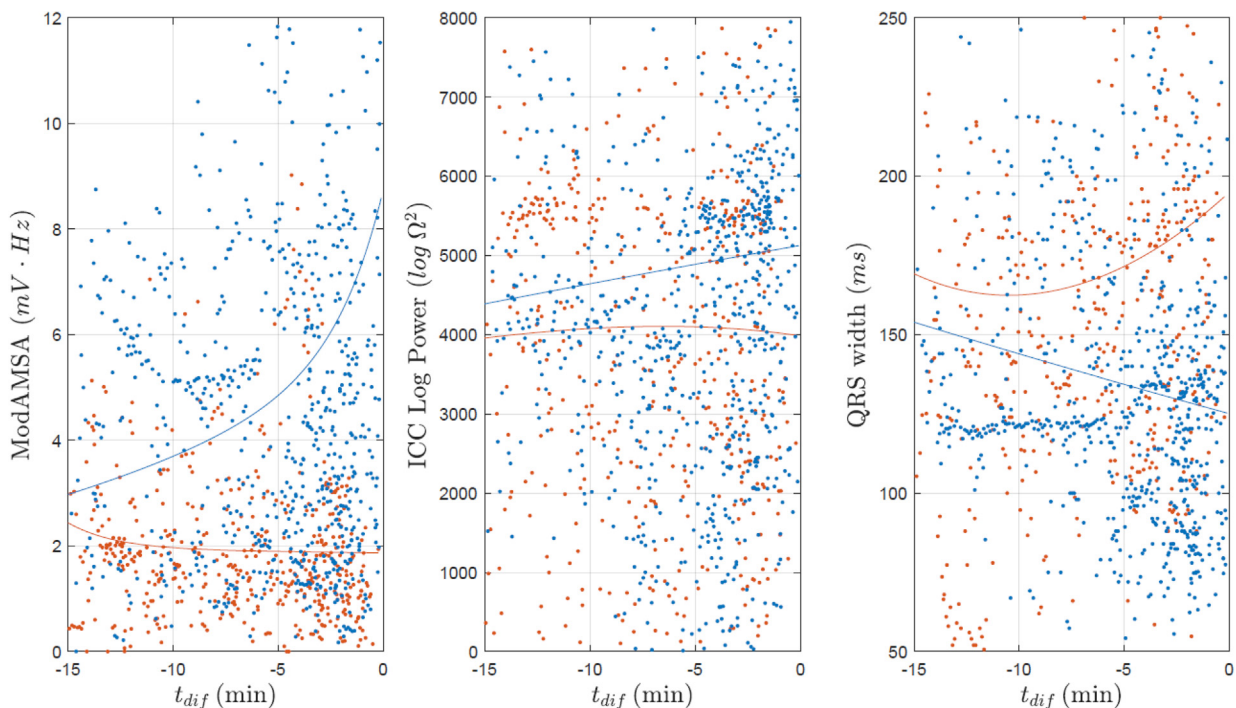
Fig. 3 – The evolution of the top three features (ModAMSA, *ICCLogPower*, and *QRSwidth*) is shown in the figure, representing the last 15 minutes before the ROSC/end-of-episode. Blue and red dots represent the feature values for faPEA and unPEA cases, respectively. The fitted exponential line is also shown for each group.

respective group. This can explain the reason behind the selection of those features. Adding new features does not include relevant information in the model, probably because they are correlated with features already present in the model, as seen for ARB_{ECG} (Pearson correlation coefficient of 0.78 with ModAMSA) and for QRS_{width} (Pearson correlation coefficient of 0.76 with QR_{width}). The correlation matrix can be found in Appendix C.

Another critical consideration lies in the database's heterogeneity. In this context, it is noteworthy that 83 entries originate from Norway, while 114 emanate from Pennsylvania. Beyond mere geographical disparities, distinctions exist in the types of defibrillator equipment utilized and the dates of data collection, potentially engendering divergent treatment modalities. To ascertain the consequential influence of these factors, Appendix D delineates the model's performance across each country. The analysis demonstrated a good performance of the model for both cases (AUC $\approx$ 80% and BAC $\approx$ 75%) and did not reveal a significant difference between them ($p > 0.05$ for both AUC and BAC). Nevertheless, to comprehensively validate the model's robustness, further experimentation incorporating additional countries and diverse defibrillator apparatuses is warranted.

When comparing the results with similar studies with OHCA,[9] the proposed algorithm performed 5.4-points below the AUC of the best OHCA models. We believe that in-hospital patients' condition might have contributed to this difference. as they are probably affected by other illness or injuries that jeopardize the design of PEA evolution models based exclusively in biosignals. Extra information as clinical/demographic data might contribute to build more complex and accurate predictive models.

Assessment of the patient's response to therapy is crucial in cardiac arrest resuscitation. Many contributions highlight the need of short-time prognosis tools that may assist clinicians in decision making.[10,19] With a favorable prognosis, it is reasonable to continue the ongoing efforts quite unaltered. However, with unfavorable prognosis, one may re-assess the situation from a broad perspective including CPR quality, and/or identification of reversible causes. Further research and prospective studies are needed to address the implications of integrating these tools into clinical practice.

Limitations of the study

The annotation of the QRS complexes to obtain the QRS-features included in the automated model was performed manually by medical experts reviewing the signals with an ad-hoc tool.

Although a completely automated method is desired, existing algorithms for QRS complex delineation were developed for stable patients and are not accurate for patients in cardiac arrest.[39,48–51] Further research is needed to overcome this limitation and develop QRS delineation algorithms robust enough in emergency scenarios.

Conclusions

A machine learning model was characterized to predict the evolution of PEA rhythms in cardiac arrest patient. The innovative LR model included features from the ECG and the TTI, with QRS-specific metrics that boosted the accuracy of the model. This new approach, evaluated with patients in IHCA, contributes to improve our knowledge on biosignal based predictive models in the field of resuscitation.

Ethical Considerations

The study is purely observational and involved no experimental intervention. Data were recorded by defibrillators used by the emergency teams responding to in-hospital emergencies and supplemented by clinical information after each event. Ethical approval was granted by the University of Pennsylvania IRB #7 for the US sites (Sept. 6th, 2017, PROTOCOL # 828086) and the regional committee for medical ethics in Central ("Midt") Norway (ref. 2019/785).

CRediT authorship contribution statement

Jon Urteaga: Writing – review & editing, Writing – original draft, Supervision, Software, Investigation, Data curation, Conceptualization. **Andoni Elola:** Writing – review & editing, Writing – original draft, Supervision, Software, Investigation, Data curation, Conceptualization. **Anders Norvik:** Writing – review & editing, Data curation, Conceptualization. **Eirik Unneland:** Writing – review & editing, Investigation, Conceptualization. **Trygve Christian Eftestøl:** Writing – review & editing, Investigation, Conceptualization. **Abhishek Bhardwaj:** Writing – review & editing, Investigation, Conceptualization. **David Buckler:** Writing – review & editing, Investigation, Conceptualization. **Benjamin S. Abella:** Writing – review & editing, Investigation, Data curation, Conceptualization. **Eirik Skogvoll:** Writing – review & editing, Investigation, Conceptualization. **Elisabete Aramendi:** Writing – review & editing, Supervision, Investigation, Data curation, Conceptualization.

Declaration of competing interest

The authors declare that they have no known competing financial interests or personal relationships that could have appeared to influence the work reported in this paper.

Acknowledgments

Appendix A. Supplementary data

Supplementary data to this article can be found online at https://doi.org/10.1016/j.resplu.2024.100598.

Author details

^{a}Communications Engineering Department, University of the Basque Country (UPV/EHU), Plaza Ingeniero Torres Quevedo 1, 48013 Bilbao, Spain^{b}Department of Electronic Technology, University of the Basque Country (UPV/EHU), Plaza Ingeniero Torres Quevedo 1, 48013 Bilbao, Spain^{c}Department of Circulation and Medical Imaging, Norwegian University of Science and Technology (NTNU), Prinsesse Kristinas gate 3, 7030 Trondheim, Norway^{d}Department of Electrical

Engineering and Computer Science, University of Stavanger (UiS), Kjell Arholms gate 41, 4021 Stavanger, Norway   ^eUniversity of California, 900 University Ave, Riverside, CA 92521, United State ^fIcahn School of Medicine at Mount Sinai, 1 Gustave L. Levy Pl, New York, NY 10029, United State^gUniversity of Pennsylvania, Philadelphia, PA 19104, United State   ^hBiocruces Bizkaia Health Research Institute, Cruces Plaza, 48903 Barakaldo, Spain

REFERENCES

1. Ko DT, Qiu F, Koh M, et al. Factors associated with out-of-hospital cardiac arrest with pulseless electric activity: a population-based study. Am Heart J 2016;177:129–37.

2. Mader TJ, Nathanson BH, Millay S, Coute RA, Clapp M, McNally B. Out-of-hospital cardiac arrest outcomes stratified by rhythm analysis. Resuscitation 2012;83:1358–62.

3. Meaney PA, Nadkarni VM, Kern KB, Indik JH, Halperin HR, Berg RA. Rhythms and outcomes of adult in-hospital cardiac arrest. Crit Care Med 2010;38:101–8.

4. Girotra S, Nallamothu BK, Spertus JA, Li Y, Krumholz HM, Chan PS. Trends in survival after in-hospital cardiac arrest. N Engl J Med 2012;367:1912–20.

5. Cobb LA, Fahrenbruch CE, Olsufka M, Copass MK. Changing incidence of out-of-hospital ventricular fibrillation, 1980–2000. JAMA 2002;288:3008–13.

6. Herlitz J, Andersson E, Bang A, et al. Experiences from treatment of out-of-hospital cardiac arrest during 17 years in Goteborg. Eur Heart J 2000;21:1251–8.

7. Norvik A, Unneland E, Bergum D, et al. Pulseless electrical activity in in-hospital cardiac arrest–A crossroad for decisions. Resuscitation 2022;176:117–24.

8. Mehta C, Brady W. Pulseless electrical activity in cardiac arrest: electrocardiographic presentations and management considerations based on the electrocardiogram. Am J Emerg Med 2012;30:236–9.

9. Urteaga J, Aramendi E, Elola A, Irusta U, Idris A. A machine learning model for the prognosis of pulseless electrical activity during out-of-hospital cardiac arrest. Entropy 2021;23:847.

10. Norvik A, Skjeflo GW, Unneland E, et al. heart rate and QRS duration predict immediate outcome in pulseless electrical activity (PEA) during in-hospital cardiac arrest (IHCA). Circulation 2022;146: A250–A.

11. Rabjohns J, Quan T, Boniface K, Pourmand A. Pseudo-pulseless electrical activity in the emergency department, an evidence based approach. Am J Emerg Med 2020;38:371–5.

12. Van den Bempt S, Wauters L, Dewolf P. Pulseless electrical activity: detection of underlying causes in a prehospital setting. Med Princ Pract 2020.

13. Rabjohns J, Quan T, Boniface K, Pourmand A. Pseudo-pulseless electrical activity in the emergency department, an evidence based approach. Am J Emerg Med 2019.

14. Myerburg RJ, Halperin H, Egan DA, et al. Pulseless electric activity: definition, causes, mechanisms, management, and research priorities for the next decade: report from a National Heart, Lung, and Blood Institute workshop. Circulation 2013;128:2532–41.

15. Flato UAP, Paiva EF, Carballo MT, Buehler AM, Marco R, Timerman A. Echocardiography for prognostication during the resuscitation of intensive care unit patients with non-shockable rhythm cardiac arrest. Resuscitation 2015;92:1–6.

16. Prosen G, Krizmaric M, Zavrsnik J, Grmec S. Impact of modified treatment in echocardiographically confirmed pseudo-pulseless electrical activity in out-of-hospital cardiac arrest patients with constant end-tidal carbon dioxide pressure during compression pauses. J Int Med Res 2010;38:1458–67.

17. Chen JY, Huang CH, Chen WJ, et al. QRS duration predicts outcomes in cardiac arrest survivors undergoing therapeutic hypothermia. Am J Emerg Med 2021;50:707–12.

18. Skjeflo GW, Nordseth T, Loennechen JP, Bergum D, Skogvoll E. ECG changes during resuscitation of patients with initial pulseless electrical activity are associated with return of spontaneous circulation. Resuscitation 2018;127:31–6.

19. Norvik A, Kvaløy J, Skjeflo G, et al. Heart rate and QRS duration as biomarkers predict the immediate outcome from pulseless electrical activity. Resuscitation 2023;185 109739.

20. Alonso E, Eftestøl T, Aramendi E, Kramer-Johansen J, Skogvoll E, Nordseth T. Beyond ventricular fibrillation analysis: comprehensive waveform analysis for all cardiac rhythms occurring during resuscitation. Resuscitation 2014;85:1541–8.

21. Lasa H, Irusta U, Eftestol T, et al. Multimodal Biosignal Analysis Algorithm for the Classification of Cardiac Rhythms During Resuscitation. In 2020 Computing in Cardiology. IEEE, 2020, 1–4

22. Elola A, Aramendi E, Irusta U, Berve PO, Wik L. Multimodal algorithms for the classification of circulation states during out-of-hospital cardiac arrest. IEEE Trans Biomed Eng 2020;68:1913–22.

23. Bhat SK, Acosta D, Swartz CM. Postictal asystole during ECT. J ECT 2002;18:103–6.

24. Burd J, Kettl P. Incidence of asystole in electroconvulsive therapy in elderly patients. Am J Geriatr Psychiat 1998;6:203–11.

25. Brown DC, Lewis AJ, Criley JM. Asystole and its treatment: the possible role of the parasympathetic nervous324 system in cardiac arrest. J Am College Emerg Phys 1979;8:448–52.

26. Losert H, Risdal M, Sterz F, et al. Thoracic-impedance changes measured via defibrillator pads can monitor signs of circulation. Resuscitation 2007;73:221–8.

27. Chicote B, Irusta U, Aramendi E, et al. Evolution of AMSA for shock success prediction during the pre-shock pause. Resuscitation 2015;96:21–2.

28. Ristagno G, Mauri T, Cesana G, et al. Amplitude spectrum area to guide defibrillation: a validation on 1617 patients with ventricular fibrillation. Circulation 2015;131:478–87.

29. Reynolds JC, Salcido DD, Menegazzi JJ. Correlation between coronary perfusion pressure and quantitative ECG waveform measures during resuscitation of prolonged ventricular fibrillation. Resuscitation 2012;83:1497–502.

30. Chicote B, Irusta U, Aramendi E, et al. Nonlinear energy operators for defibrillation shock outcome prediction. In 2016 Computing in Cardiology Conference (CinC). IEEE, 2016, 61–64

31. El Bouny L, Khalil M, Abdellah AQRS, complex detection based on smoothed nonlinear energy operator. In,. 9th International symposium on signal, image, video and communications (ISIVC). IEEE 2018;2018:191–6.

32. Bos R, De Waele S, Broersen PM. Autoregressive spectral estimation by application of the Burg algorithm to irregularly sampled data. IEEE Trans Instrum Meas 2002;51:1289–94.

33. Rad AB, Eftestøl T, Engan K, et al. ECG-based classification of resuscitation cardiac rhythms for retrospective data analysis. IEEE Trans Biomed Eng 2017;64:2411–8.

34. Elola A, Aramendi E, Irusta U, Del Ser J, Alonso E, Daya M. ECG-based pulse detection during cardiac arrest using random forest classifier. Med Biol Eng Compu 2019;57:453–62.

35. Ruiz JM, de Gauna SR, Gonzalez-Otero DM, et al. Circulation assessment by automated external defibrillators during cardiopulmonary resuscitation. Resuscitation 2018;128:158–63.

36. Alonso E, Aramendi E, Daya M, et al. Circulation detection using the electrocardiogram and the thoracic impedance acquired by defibrillation pads. Resuscitation 2016;99:56–62.

37. Elola A, Aramendi E, Irusta U, et al. ECG characteristics of pulseless electrical activity associated with return of spontaneous circulation in out-of-hospital cardiac arrest. Resuscitation 2018;130:e54.

38. Elola A, Aramendi E, Irusta U, et al. Capnography: A support tool for the detection of return of spontaneous circulation in out-of-hospital cardiac arrest. Resuscitation 2019;142:153–61.

39. Bergum D, Skjeflo GW, Nordseth T, et al. ECG patterns in early pulseless electrical activity-associations with aetiology and survival of in-hospital cardiac arrest. Resuscitation 2016;104:34–9.

40. Kim JH, Ryoo HW, Jy K, et al. QRS complex characteristics and patient outcomes in out-of-hospital pulseless electrical activity cardiac arrest. Emerg Med J 2021;38:53–8.

41. Aufderheide TP, Thakur RK, Stueven HA, et al. Electrocardiographic characteristics in EMD. Resuscitation 1989;17:183–93.

42. Weiser C, Poppe M, Sterz F, et al. Initial electrical frequency predicts survival and neurological outcome in out of hospital cardiac arrest patients with pulseless electrical activity. Resuscitation 2018;125:34–8.

43. Jekova I, Krasteva V. Real time detection of ventricular fibrillation and tachycardia. Physiol Meas 2004;25:1167.

44. Ristagno G, Gullo A, Berlot G, Lucangelo U, Geheb F, Bisera J. Prediction of successful defibrillation in human victims of out-of-hospital cardiac arrest: a retrospective electrocardiographic analysis. Anaesth Intensive Care 2008;36:46–50.

45. Indik JH, Conover Z, McGovern M, et al. Association of amplitude spectral area of the ventricular fibrillation waveform with survival of out-of-hospital ventricular fibrillation cardiac arrest. J Am Coll Cardiol 2014;64:1362–9.

46. Raymond TT, Pandit SV, Griffis H, et al. Effect of amplitude spectral area on termination of fibrillation and outcomes in pediatric cardiac arrest. J Am Heart Assoc 2021;10:e020353.

47. Gentile FR, Wik L, Isasi I, et al. Amplitude spectral area of ventricular fibrillation and defibrillation success at low energy in out-of-hospital cardiac arrest. Intern Emerg Med 2023:1–9.

48. Martínez JP, Almeida R, Olmos S, Rocha AP, Laguna P. A wavelet-based ECG delineator: evaluation on standard databases. IEEE Trans Biomed Eng 2004;51:570–81.

49. Shaik BS, Naganjaneyulu G, Chandrasheker T, Narasimhadhan A. A method for QRS delineation based on STFT using adaptive threshold. Procedia Comput Sci 2015;54:646–53.

50. Teijeiro T, Félix P, Presedo J. A noise robust QRS delineation method based on path simplification. In 2015 Computing in Cardiology Conference (CinC). IEEE, 2015, 209–212

51. Berkaya SK, Uysal AK, Gunal ES, Ergin S, Gunal S, Gulmezoglu MB. A survey on ECG analysis. Biomed Signal Process Control 2018;43:216–35.